

Received June 22, 2018, accepted July 17, 2018, date of publication July 24, 2018, date of current version August 15, 2018.

Digital Object Identifier 10.1109/ACCESS.2018.2859359

How Do Detected Objects Affect the Noise Distribution of Terahertz Security Images?

ZHAODI WANG¹, MENGHAN HU^{1,2}, ERCAN ENGIN KURUOGLU³, (Senior Member, IEEE),
WENHAN ZHU¹, AND GUANGTAO ZHAI¹, (Member, IEEE)

¹Institute of Image Communication and Information Processing, Shanghai Jiao Tong University, Shanghai 200240, China

²Shanghai Key Laboratory of Multidimensional Information Processing, East China Normal University, Shanghai 200241, China

³Institute of Science and Technology of Information, "A. Faedo," CNR, National Council of Research of Italy, 56124 Pisa, Italy

Corresponding authors: Menghan Hu (humenghan89@163.com), Ercan Engin Kuruoglu (ercan.kuruoglu@isti.cnr.it), and Guangtao Zhai (zhai Guangtao@sjtu.edu.cn)

This work was supported in part by the China Postdoctoral Science Foundation under Project 2016M600315, in part by the National Science Foundation of China under Grant 61521062 and Grant 61527804, and in part by the Equipment Pre-research Joint Research Program of Ministry of Education under Grant 6141A020223.

ABSTRACT The purpose of this paper is to analyze how detected objects affect the noise distribution of terahertz (THz) security images. Noise in THz image caused by hardware deteriorates the image quality seriously, limiting the application. In addition, there are a few papers on the noise analysis of THz screenings. Due to the special attributes of the THz image compared with the natural image, an alpha-stable distribution is used to fit the noise of THz image instead of the commonly-used Gaussian distribution. The database used in this paper is composed of 181 THz image cubes with a test object as well as two empty image cubes. After analyzing the four parameters of alpha-stable distribution, we can observe that the noise patterns of THz images are indeed different from those of natural image obtained by RGB camera. The possible reasons are given based on the principles of the THz imaging device. The analysis of the distribution of four parameters of alpha-stable model demonstrates that there exists a nonlinear effect due to the change of reflected wave's pattern caused by the body structure. This paper provides an efficient and flexible model for THz images and a useful guidance for the design of THz image denoising algorithms and the development of imaging hardware.

INDEX TERMS THz image, noise pattern, noise estimation, statistical analysis, alpha-stable distribution.

I. INTRODUCTION

THz radiation generally refers to the frequency band between the microwave and infrared regions of the electromagnetic spectrum [1]. This spectral region was not fully explored for a long time in scientific history. With the development of terahertz (THz) source generator and detector, the "THz gap" has been bridged and THz imaging technique has aroused more and more concerns in various applications [2] such as biological diagnosis [3], security inspection [4], authentication of electronic components [5], counterfeit detection and quality inspection [6], [7]. Due to the two prominent advantages of THz imaging technique, compared to the other imaging methods, viz. low photon energy and high transparency, THz imaging technique has been extensively used for both military and civilian purposes. With respect to security application scenarios, the use of THz imaging device stands out for the reason that the THz waves can penetrate through most uncharged substances, which allows us to detect the concealed illegal materials [8].

To date, most current THz imaging devices are equipped with low-stability sources at insufficient power levels and conduct one scan with several seconds. Hence, the quality of ultimate THz data is highly affected by the changes of environmental factors and the operation conditions of equipment [9]. This will further deteriorate the detection performance (because of loss of detected structures) and even hamper the extension of THz imaging technique to the large scale applications. After observing the THz images, we can find that the main distortion type for THz images is their high noise level [10]. Some research work is dedicated to develop de-noising algorithms to attenuate the noise brought by the factors mentioned above [11]. Yue *et al.*, leveraged Wiener filter, gray stretch algorithm and genetic algorithm to smooth the THz security images [12]. They did not point out why they chose Wiener filter. Trofimov and Trofimov [13] selected the image characteristics from the reference image to create the correlation function for suppress noise in THz image. Ahi and Anwar [14] introduced a novel reconstruction

approach for enhancing the resolution of the THz images, including the scene that the signal drops exponentially to the noise floor with respect to the thickness of the object and frequency of the THz beam. Reference image is the image containing no or little noise, which is difficult to find or define. Liu and Li [15] used the adaptive threshold de-noising algorithm derived from the Bayesian approach to reduce noise in THz image. This adaptive threshold de-noising algorithm is unsuitable for removing background noise. To the best of our knowledge, there is no publication on analyzing the noise pattern in THz images. The first step into designing noise elimination methods is to understand the statistical characteristics of the noise on THz images.

Therefore, understanding of noise pattern will also provide useful guidance for the design of terahertz imaging hardware. Currently, analysis of noise characteristics is commonly studied for natural image obtained by RGB camera [16], [17]. In respect to noise estimation of specific image modalities, Goodall *et al.*, concluded that noise in thermal images is an additive fixed-pattern, and they stated that this stripe noise profile is specific to thermal images [18]. This inspires us to explore the noise statistical characteristic of THz image. For noise estimation of THz signal, some investigations had been carried out on THz spectral signal [19]. The random noise had been considered as the major error source of THz spectra, which is approximately 1% of the signal intensity [20]. Naftaly used the Fourier transform for original THz spectrum to acquire the noise signal [21]. No related work has been conducted on the statistical analysis of THz image noise.

Consequently, our objective in this paper is to analyze how detected objects affect the noise distribution of THz security images. We propose the use of alpha-stable distributions for modelling pixel distribution of terahertz images and provide experimental results verifying our hypothesis.

II. THz IMAGING EQUIPMENT AND DATA STRUCTURE OF THz IMAGE

A. IMAGING EQUIPMENT AND ITS OPERATING PRINCIPLE

Before analyzing the noise distribution of the THz image, the operating principle of imaging device must be figured out.

Fig. 1 shows the operating principle of active THz reflectance imaging device. THz wave is generated by a THz wave generator, and THz reflectance signals are recorded by a THz wave detector. The THz wave generator and detector are integrated into a plate on the same side of testing person. Such active THz imaging device is configured to separate the detection space into 200 subsections, and the THz reflectance signals of each subsection are captured by the THz detector. In terms of every scan, one three-dimensional (3-D) data can be obtained, which is called image cube in this research. The structure of this 3-D THz cube will be elaborated in the following text.

The effective measurement height of the device ranges from 0.15 m to 2.00 m. Scanning time is less than 3 seconds.

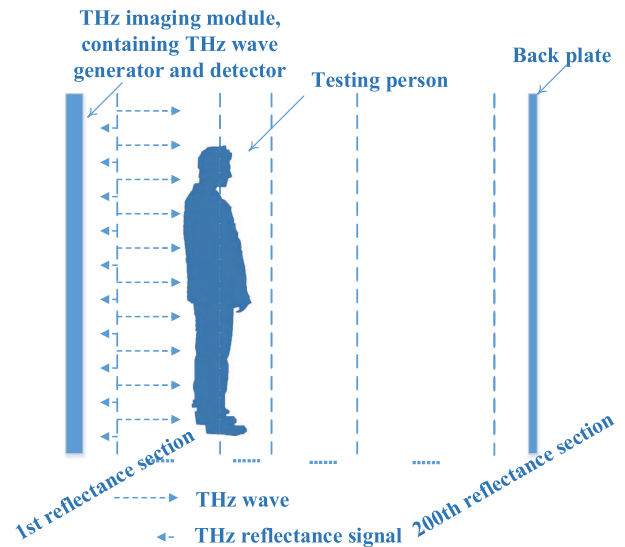


FIGURE 1. The operating principle of active THz reflectance imaging device. The imaging device in this research was configured to separate the detection space into 200 subsections.

The imaging device is a custom-made Transmit/Receive (T/R) module which operates in active reflection imaging mode, offering line resolution of less than 2 mm, and spatial resolution of less than 6 mm.

B. THz IMAGE DATABASE

In the previous study, we have constructed the THz security image database (THSID) [10]. Four volunteers were invited to generate THSID. Each time they were imaged in the device with various illegal materials such as hammer and knife, or with some legal materials such as belt and soap. THSID contains 181 sets of THz security images.

In order to describe the noise distribution of THz image without object, we also collected two image cube with no testing person in.

C. THz IMAGE STRUCTURE

Fig. 2 shows an example of THz security image cube in THSID. The raw THz security image cube is three-dimensional with X-, Y- and Z-axes. We split each 3-D image cube to 200 two-dimensional images with resolution of 127×380 and call such 2-D image as “slice” in this work.

We can realize that the background is black while the noise and body structure is white through the above description. Pixel values are from 0 to 255 in grayscale.

III. NOISE STATISTICAL ANALYSIS OF THz IMAGE

When we understand the noise pattern in THz image, the better de-noising algorithms can be developed for improvement of THz image quality. We tried to fit the histograms of slices are skewed (lacking left tail in particular) and are heavy tailed using Gaussian distribution, but the histogram lacks a left tail, since the THz beam is not a monochromatic beam. Each frequency component of the beam has different attenuation

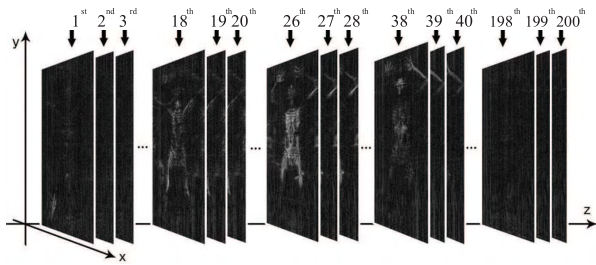


FIGURE 2. Data structure of a THz security image cube, containing 200 two-dimensional vertical image slices.

factors in the object [22]. Thus, the noise distribution of a THz image is different from that of a natural image obtained by RGB camera. We then considered a more general distribution, namely the alpha-stable distribution.

A. NOISE STATISTICAL ANALYSIS OF DIFFERENT KINDS OF 2D THz IMAGE SLICES

Motivated by the popularity of alpha stable distributions in modelling impulsive and skewed phenomenon [23], we attempted to fit the histogram of each slice by an alpha-stable distribution. The characteristic function of alpha-stable distribution is defined as:

$$\varphi(t; \alpha, \beta, \gamma, \delta) = e^{it\delta - |\gamma t|^\alpha (1 - i\beta \text{sgn}(t)\Phi)} \tag{1}$$

where

$$\Phi = \begin{cases} \tan(\frac{\pi\alpha}{2}) & \alpha \neq 1 \\ -\frac{2}{\pi} \log |\gamma t| & \alpha = 1 \end{cases} \tag{2}$$

α, β, γ and δ are four parameters of the alpha-stable distribution, representing stability, skewness, scale and location, respectively.

In order to find out whether the object in the THz imaging device affects the noise distribution, we contrasted models fit to the histograms of slices at different positions. Slices were grouped into four types, namely slices in the empty cube, slices with body structure, slices near the edge of the body structure (within 10 slices from the edge of body structure) and slices far away from the body structure (more than 10 slices from the edge of body structure). Description about the last three kinds of slices are presented in Fig. 3.

For the sake of analyzing the noise space distribution, we tried to identify the range of projections of body structure on the Z-axis. Contrast stretch transformation [24], an image enhancement method using nonlinear grayscale transformation, is applied to enhance the difference between slices with and without body structure. After analyzing the histogram of each slice, we pick out continuous slices that the number of pixels whose value under 20 account for 90% or higher as the range of the body structure along Z-axis [25].

Fig. 4 shows the probability distribution function (PDF) and cumulative distribution function (CDF) of all the slices in the empty image cube and slices with body structure.

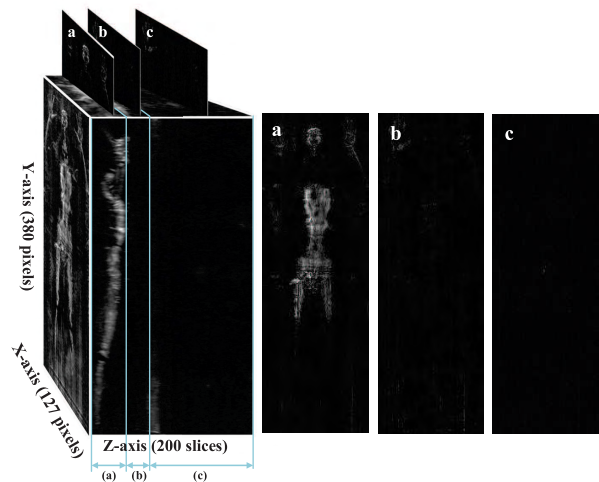


FIGURE 3. Description about slices in the image cube with a person: (a) slices with body structure; (b) slices near the edge of the body structure; (c) slices far away from the body structure.

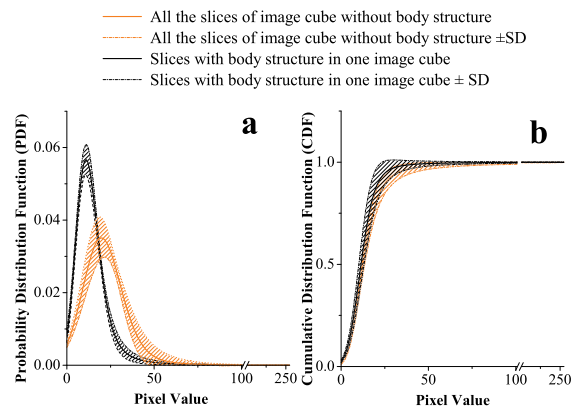


FIGURE 4. Average PDF and CDF of all the slices in image cube without person and slices with body structure.

The PDF in Fig. 4 (a) demonstrates a great difference between the two curves. Theoretically, slices in image cube without object is all black, that is, pixel value should all be 0. However, due to the influence of environmental factors (e.g. temperature and humidity) and the unstable performance of imaging device, there exist some pixels not equal to 0 in THz image. As shown in Fig. 4 (a), the distribution of the intensity of these pixels follows the alpha-stable distribution. Slices in image cube with body structure are also subject to alpha-stable distribution with different fitting parameters. Thus, the object in the THz imaging device does affect the noise distribution. Due to the attenuating affect of the terahertz imaging device and imaging conditions, the pixel values are limited to below 25.

It is worth discussing the distribution of the body structure as well as the way the body structure affects the noise distribution. Therefore, we will analyze the remaining two kinds of slices, namely slices near the edge of the body structure and slices far away from the body structure, to explore whether the testing objects influence the noise pattern or not.

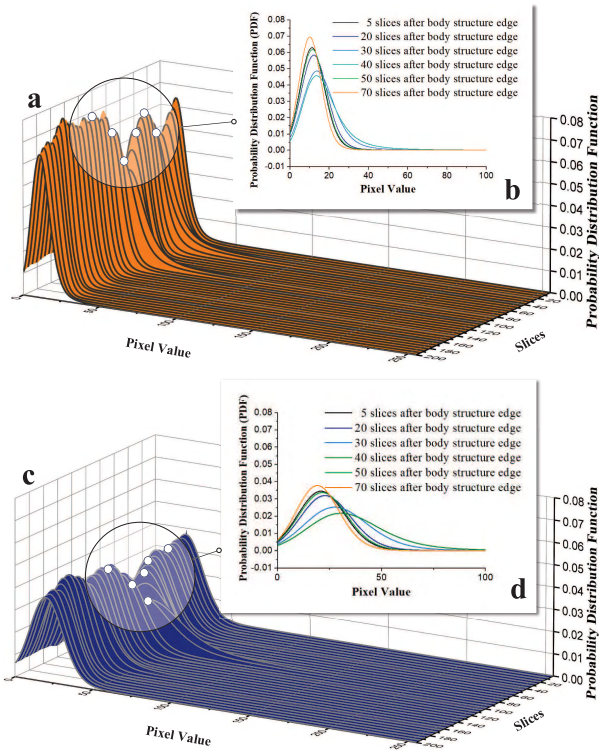


FIGURE 5. (a) In an image cube with body structure, PDF of all the slices. (b) In an image cube with body structure, PDF of slices with different distances away from the testing body edge, with horizontal scale as pixel value in the range of 0 to 100. (c) In an image cube without body structure, PDF of all the slices. (d) In an image cube without body structure, PDF of slices with same position in (b), with horizontal scale as pixel value in the range of 0 to 100.

Fig. 5 shows the difference of PDF curves among the various distances away from the edge of body structure. In the example of Fig. 5 (a) and (b), the body structure exists from slice 1 to slice 44. PDF of image slices with different distances away from the testing body edge are shown in Fig. 5 (b) and (d). The fitting values of image cube with body structure are more concentrated around smaller values than the image cube without an object. The object in the imaging device acts as a filter and suppresses the background noise to some extent. This provides an idea for us to design a noise filter specific to THz image. In addition, the THz waves are able to pass through the detected object, which can be seen in Fig. 5. Therefore, the analysis of surviving THz waves in the slices behind the body are important in some application scenarios.

B. POSSIBLE REASONS BEHIND NOISE PATTERNS OF THz IMAGE

After analyzing noise patterns of different kinds of in THz image cube, we wondered the reasons behind these noise patterns. Hence, in this section, we explore the possible reasons via the analysis of the parameters of alpha-stable model and the principle of THz imaging.

Fig. 6 shows the four parameters’ distributions of alpha-stable model for all slices in THz image cube without body

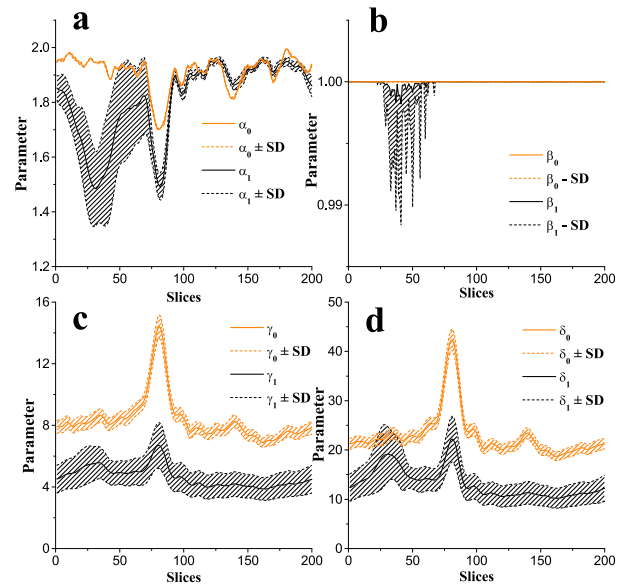


FIGURE 6. Four parameters’ distributions of alpha-stable model, where $\alpha_0, \beta_0, \gamma_0, \delta_0$ are parameters of image cube without body structure, and $\alpha_1, \beta_1, \gamma_1, \delta_1$ are parameters of image cube with body structure. In (b), since $\beta \in [-1, 1]$, only (mean - SD) are plotted. The p-values of t-test of α, β, γ and δ are 2.48e-19, 1.02e-15, 1.23e-81 and 1.40e-112, respectively.

structure (with subscript 0) and with body structure (with subscript 1). In the image cubes with person, the edge of body structure is at slice 33 to slice 105. We can infer that: (1) A sudden jump of γ and δ occurs from slice 70 to slice 90 in image cubes both without and with body structure, due to the ground noise. For α , in the same slice position for both two kinds of image cubes, there is a slight drop. Due to the stability property, the output of a linear system to an alpha-stable process is an alpha stable process with the same α while β and γ can change. A linear interaction between the noise and the object such as addition would not have changed the value of the parameter α . The fact that we see change in the value of α when there is an object tells us that the system loses its linearity and there are nonlinear interactions between the body and the measurement wave. This might be caused by the fact that the noise is multiplicative rather than additive. The effect of the device inner geometry is also evident with the appearance of a region where the α value changes in the presence of the object in the device although this region is not the interval where the body is placed. (2) Parameter γ and δ of image cube without body structure is larger than that of with one, demonstrating that the body structure reduces the noise caused by reflection in some extent. Such conclusion also can be demonstrated in Fig. 4. (3) Extra peaks of γ and δ arise of the image cube with a person, caused by the existence of body structure. The position of the peaks agrees with the position of the body structure. The sudden jump of these two parameters means that the original distribution is disturbed if the testing person enters into the THz imaging chamber. According to the previous statement of the THz imaging principle, such change can be attributed to the reflection of the waves on body

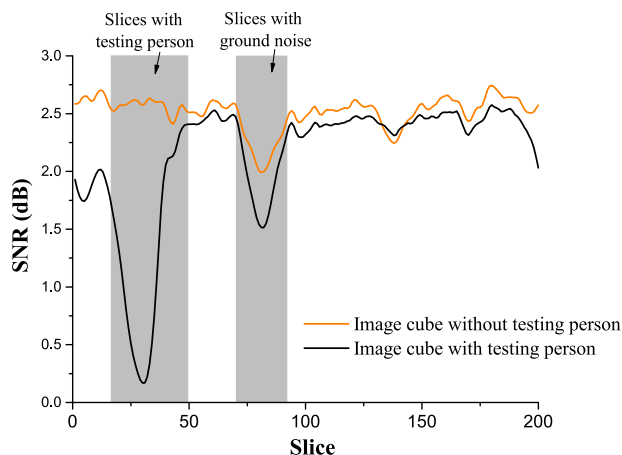


FIGURE 7. Signal-noise ratio of an image cube with testing person and one without testing person. Testing person is in slices 20 to slice 50, while ground noise exists in slice 70 to slice 90.

structure, which is a nonlinear effect. (4) Parameter β remains at 1, which means skewness of different slices is stable. (5) T-test is performed on each set of parameters. The hypothesis test results are all 1, which means the test rejects the null hypothesis at the 5% significance level. The p-values of t-test of α , β , γ and δ are $2.48e-19$, $1.02e-15$, $1.23e-81$ and $1.40e-112$, respectively, suggesting that the object in the imaging chamber will affect the noise distribution.

Same rule was found when we checked parameters' distributions of alpha-stable model of all the image cubes.

Fig. 7 shows the signal-noise ratio (SNR) of an image cube with testing person and an image cube without testing person. Testing person is in slices 20 to slice 50, while ground noise exists in slice 70 to slice 90. SNR of slices without body structure is higher than SNR of slices with body structure, which may due to the noise being non-additive.

In future study, we may take the attenuation factor and the thickness of the object into consideration (as it is described in [22]). To do that, we believe that the noise can be fitted into a new equation, which derives from the Gaussian distribution, to give the better THz noise model.

IV. CONCLUSION

In this study, we analyzed how detected objects affect the noise distribution of Terahertz security images. The operating principle of active THz reflectance imaging device and the THz image database are introduced first. Unlike the natural image obtained by RGB camera, the pixel value of the THz image does not follow the Gaussian distribution since THz beam is not a monochromatic beam. We consider a more general model, namely alpha-stable distribution. The probability distribution function curves of the slices with and without body structure show that the object in the THz imaging device does affect the noise distribution. After analyzing the distribution of four parameters of alpha-stable model, we know that there exists a nonlinear effect due to the change of reflected wave's pattern caused by body structure. This study

provides a new statistical model for the noise in THz images and demonstrates how the model parameters are affected by the object, indicating nonlinear interactions between the object and the THz waves. Method of noise reduction for three-dimensional THz image still remains to be explored. More advanced denoising algorithms could be particularly applicable to THz-TDS (THz-Time Domain Spectrometer) systems, since these systems provide the time-domain version and hence the spectrum of the THz beam. This could be considered an additional privilege of THz-TDS over RGB visible-light cameras. Based on the noise distribution characteristic of THz image presented in this study, a custom designed denoising filter can be added to the process in the future work, so that our research could be expanded to more advanced applications.

ACKNOWLEDGEMENT

The authors would like to acknowledge the staffs working in BOCOM Smart Network Technologies Inc., who assisted in acquiring the THz images. The authors would also like to acknowledge the anonymous reviewers, who gave constructive suggestions and helped to improve the manuscript greatly.

REFERENCES

- [1] X. Yang et al., "Biomedical applications of terahertz spectroscopy and imaging," *Trends Biotechnol.*, vol. 34, pp. 810–824, Oct. 2016.
- [2] Z. Popovic and E. N. Grossman, "THz metrology and instrumentation," *IEEE Trans. THz Sci. Technol.*, vol. 1, no. 1, pp. 133–144, Sep. 2011.
- [3] Q. Sun, Y. He, K. Liu, S. Fan, E. P. Parrott, and E. Pickwell-MacPherson, "Recent advances in terahertz technology for biomedical applications," *Quant. Imag. Med. Surg.*, vol. 7, no. 3, p. 345, 2017.
- [4] D. Suzuki, S. Oda, and Y. Kawano, "A flexible and wearable terahertz scanner," *Nature Photon.*, vol. 10, no. 12, pp. 809–813, 2016.
- [5] K. Ahi, N. Asadizanjani, S. Shahbazmohamadi, M. Tehranipoor, and M. Anwar, "Terahertz characterization of electronic components and comparison of terahertz imaging with X-ray imaging techniques," *Proc. SPIE*, vol. 9483, p. 94830K, May 2015.
- [6] K. Ahi, S. Shahbazmohamadi, and N. Asadizanjani, "Quality control and authentication of packaged integrated circuits using enhanced-spatial-resolution terahertz time-domain spectroscopy and imaging," *Opt. Lasers Eng.*, vol. 104, pp. 274–284, May 2018.
- [7] K. Ahi and M. Anwar, "Advanced terahertz techniques for quality control and counterfeit detection," *Proc. SPIE*, vol. 9856, p. 98560G, May 2016.
- [8] M. Polini, "Tuning terahertz lasers via graphene plasmons," *Science*, vol. 351, pp. 229–231, Jan. 2016.
- [9] L. Hou, X. Lou, Z. Yan, H. Liu, and W. Shei, "Enhancing terahertz image quality by finite impulse response digital filter," in *Proc. Int. Conf. Infr. Millim., THz Waves*, Sep. 2014, pp. 1–2.
- [10] M. Hu et al., "Terahertz security image quality assessment by no-reference model observers," in *Digital TV and Wireless Multimedia Communication*, G. Zhai, J. Zhou, and X. Yang, Eds. Singapore: Springer, 2018, pp. 100–114.
- [11] K. I. Zaytsev et al., "An approach for automatic construction of the wavelet-domain de-noising procedure for THz pulsed spectroscopy signal processing," *J. Phys., Conf. Ser.*, vol. 486, no. 1, p. 012034, 2014.
- [12] G. Yue, Z. Yu, C. Liu, H. Huang, Y. Zhu, and L. Jiang, "Identification and annotation of hidden object in human terahertz image," in *Information Science and Applications*. Singapore: Springer, 2017, pp. 155–163.
- [13] V. A. Trofimov and V. V. Trofimov, "New algorithm for the passive THz image quality enhancement," *Proc. SPIE*, vol. 9856, p. 98560M, Apr. 2016.
- [14] K. Ahi and M. Anwar, "Developing terahertz imaging equation and enhancement of the resolution of terahertz images using deconvolution," *Proc. SPIE*, vol. 9856, p. 98560N, May 2016.

- [15] J. Liu and Z. Li, "Antcolony combined with adaptive threshold denoising and reconstruct for thz image," *Optik—Int. J. Light Electron Opt.*, vol. 125, no. 14, pp. 3423–3427, 2014.
- [16] A. Khmag, A. R. Ramli, S. A. R. Al-haddad, and N. Kamarudin, "Natural image noise level estimation based on local statistics for blind noise reduction," *Vis. Comput.*, vol. 34, no. 4, pp. 575–587, 2017.
- [17] T. H. Thai, F. Retraint, and R. Cogranne, "Camera model identification based on the generalized noise model in natural images," *Digit. Signal Process.*, vol. 48, pp. 285–297, Jan. 2016.
- [18] T. R. Goodall, A. C. Bovik, and N. G. Paulter, "Tasking on natural statistics of infrared images," *IEEE Trans. Image Process.*, vol. 25, no. 1, pp. 65–79, Jan. 2016.
- [19] M. Naftaly and R. Dudley, "Methodologies for determining the dynamic ranges and signal-to-noise ratios of terahertz time-domain spectrometers," *Opt. Lett.*, vol. 34, pp. 1213–1215, Apr. 2009.
- [20] E. Bründermann, H.-W. Hübers, and M. F. Kimmitt, *Terahertz Techniques*, vol. 151. Berlin, Germany: Springer, 2012.
- [21] M. Naftaly, "Metrology issues and solutions in THz time-domain spectroscopy: Noise, errors, calibration," *IEEE Sensors J.*, vol. 13, no. 1, pp. 8–17, Jan. 2013.
- [22] K. Ahi, "Mathematical modeling of THz point spread function and simulation of THz imaging systems," *IEEE Trans. THz Sci. Technol.*, vol. 7, no. 6, pp. 747–754, Nov. 2017.
- [23] G. R. Arce, *Nonlinear Signal Processing: A Statistical Approach*. Hoboken, NJ, USA: Wiley, 2005.
- [24] R. C. Gonzalez and R. E. Woods, *Digital Image Processing*. Englewood Cliffs, NJ, USA: Prentice-Hall, 2002.
- [25] Z. Wang, M. Hu, W. Zhu, X. Yang, and G. Tian, "Selection of good display mode for terahertz security image via image quality assessment," in *Digital TV and Wireless Multimedia Communication*, G. Zhai, J. Zhou, and X. Yang, Eds. Singapore: Springer, 2018, pp. 277–289.



ERCAN ENGIN KURUOGLU (M'98–SM'06) received the M.Phil. and Ph.D. degrees in information engineering from the University of Cambridge, Cambridge, U.K., in 1995 and 1998, respectively. In 1998, he joined the Collaborative Multimedia Research Laboratory, Xerox Research Center Europe, Cambridge. He was an ERCIM Fellow with INRIA-Sophia Antipolis, France, in 2000. In 2002, he joined ISTI-CNR, Pisa, Italy, as a Permanent Member. He was a Visiting Professor with Georgia Tech-China in 2007, 2011, and 2016 and with the Southern University of Science and Technology of China, Shenzhen, in 2017. He was an Alexander von Humboldt Experienced Research Fellow with the Department of Theoretical Biophysics, Humboldt University, in 2012, and with the Max Planck Institute for Molecular Genetics from 2013 to 2014. He is currently a Senior Researcher at ISTI-CNR. His research interests are in the areas of statistical signal and image processing and information and coding theory with applications in computational biology, telecommunications, earth sciences, and astrophysics. He is a member of the IEEE Technical Committee on Signal Processing Theory and Methods. He acted as a Technical Co-Chair for EUSIPCO 2006 and a Tutorials Co-Chair of ICASSP 2014. He was a Plenary Speaker at ISSPA 2010, the IEEE SIU 2017, and Entropy 2018, and a Tutorial Speaker at the IEEE ICSPCC 2012. He was a Chinese Government 111 Project Foreign Expert from 2007 to 2011. He was an Associate Editor of the IEEE TRANSACTIONS ON SIGNAL PROCESSING and the IEEE TRANSACTIONS ON IMAGE PROCESSING. He is currently an Editor-in-Chief of *Digital Signal Processing: A Review Journal*.



WENHAN ZHU received the B.E. degree from the School of Huazhong University of Science and Technology, Wuhan, China, in 2015. He is currently pursuing the Ph.D. degree with the Institute of Image Communication and Information Processing, Shanghai Jiaotong University, Shanghai, China.



GUANGTAO ZHAI (M'10) received the B.E. and M.E. degrees from Shandong University, Shandong, China, in 2001 and 2004, respectively, and the Ph.D. degree from Shanghai Jiao Tong University, Shanghai, China, in 2009.

From 2008 to 2009, he was a Visiting Student with the Department of Electrical and Computer Engineering, McMaster University, Hamilton, ON, Canada, where he was a Post-Doctoral Fellow from 2010 to 2012. From 2012 to 2013, he was a Humboldt Research Fellow with the Institute of Multimedia Communication and Signal Processing, Friedrich Alexander University of Erlangen-Nuremberg, Germany. He is currently a Research Professor with the Institute of Image Communication and Information Processing, Shanghai Jiao Tong University. His research interests include multimedia signal processing and perceptual signal processing. He received the Award of National Excellent Ph.D. Thesis from the Ministry of Education of China in 2012.

...



ZHAODI WANG received the B.E. degree from the School of Information Science and Technology, Southeast University, Nanjing, China, in 2017. She is currently pursuing the degree with the Institute of Image Communication and Information Processing, Shanghai Jiao Tong University, Shanghai, China.



MENGHAN HU received the Ph.D. degree (Hons.) in biomedical engineering from the University of Shanghai for Science and Technology in 2016. From 2016 to 2018, he was a Post-Doctoral Researcher with Shanghai Jiao Tong University. He is currently an Associate Professor with the Shanghai Key Laboratory of Multidimensional Information Processing, East China Normal University.